Original Article

Posterior corneal morphological changes in primary congenital glaucoma

Shikha Gupta, Karthikeyan Mahalingam, Abhishek Singh, Harathy Selvan, Bindu I Somarajan, Viney Gupta

Purpose: To compare posterior corneal morphology between older treated and younger untreated children with primary congenital glaucoma (PCG) using anterior segment optical coherence tomography (ASOCT) and intraoperative OCT (iOCT), respectively. **Methods:** In this comparative study, ASOCT of older PCG children were compared with iOCT of younger untreated PCG patients. Differences between the two groups with respect to posterior corneal morphology were studied. **Results:** Observed morphological patterns within posterior cornea in older treated (age: 72–300 months) children (87 eyes) included Descemet's membrane (DM) excrescences (70%), thickened DM (35%), intracameral twin protuberances (92%), and DM detachment (26%). Changes within pre-Descemet's layer (PDL) (28%) included thickening, breaks, and detachments. Extent of Haab's striae was associated with thickness of DM/PDL complex (P = 0.008) when analyzed in the treated group. In contrast, in the untreated group (n = 53 eyes, age 1–63 months), posterior corneal changes were limited to diffuse hyper-reflectivity of the DM/PDL complex, with absence of DM tears. **Conclusion:** Posterior cornea thickens and Haab's striae become more circumscribed in eyes of older treated children compared to untreated PCG eyes, probably reflecting a healing response of posterior cornea over time.

Access this article online

Website: www.ijo.in

DOI: 10.4103/ijo.IJO_317_22

Quick Response Code:

Key words: Anterior Segment Optical Coherence Tomography, congenital glaucoma, Descemet's membrane, Haab's striae, pre-Descemet's membrane

The Descemet's membrane (DM) is an elastic basement membrane which is continuously secreted by the corneal endothelium and is made up of collagen, laminin, and fibronectin.[1] It aids in distributing the corneal tension uniformly, thus preventing its deformation. Being elastic in nature, it curls onto itself when severed or when its elasticity is surpassed. Tears in DM secondary to intraocular pressure (IOP)-induced corneal stretching in primary congenital glaucoma (PCG) cases have been typically referred to as Haab's striae. However, tears in DM can also occur in acute hydrops, following cataract surgery in cases with DM detachment, and after birth trauma.[2-4] Haab's striae are often considered an indisputable sign of PCG. It is accompanied by edema, which may eventually settle down if the gap gets sealed, or it may progress to permanent stromal scarring in cases of persistent edema.[5]

Haab's striae, on slit lamp, have a characteristic rail-track appearance.[6] Benito-Pascual *et al*.[7] described three cases of PCG with Haab's striae, seen as focal excrescences on anterior segment optical coherence tomography (ASOCT). With the advent of high-definition spectral domain optical coherence tomography (SDOCT), *in vivo* differentiation of pathology within selective corneal layers has become more achievable. Unfortunately, there are only a few studies that have characterized the morphology of Haab's striae in detail.[6-10] This study aimed to observe and compare the posterior corneal morphological features between older treated and younger untreated children with PCG, especially with regards to the Haab's striae. This will help us to derive the impact of IOP on posterior corneal healing.

Methods

In this observational study, we recruited PCG patients within two arms, the older treated group and the younger untreated group. Only one eye of each patient was randomly chosen using computer-generated software for the study. Approval from the Institutional Ethics Committee was obtained, and the study adhered to the tenets of Declaration of Helsinki. Written informed consent was obtained from the guardian of each participant or the adult participants themselves for the study.

Treated PCG

Consecutive treated PCG patients, following up at the glaucoma clinic of our tertiary care center during Jan 2019–Dec 2020 and cooperative for clinical examination and ASOCT imaging, were included. Patients with secondary glaucoma, nystagmus, those with intraoperative complications leading to DM tears, and those with poor fixation were excluded from the study.

Details of current age, gender, treated IOP on follow-up (Goldmann applanation/Perkin's tonometer;

Glaucoma Services, Dr Rajendra Prasad Centre for Ophthalmic Sciences, All India Institute of Medical Sciences, New Delhi, India

Correspondence to: Dr. Shikha Gupta, Associate Professor, Glaucoma Services, Dr. Rajendra Prasad Centre for Ophthalmic Sciences, All India Institute of Medical Sciences, New Delhi – 110 029, India. E-mail: shikhagupta@aiims.edu

Received: 10-Mar-2022 Revision: 08-Apr-2022
Accepted: 04-Jun-2022 Published: 30-Jun-2022

Cite this article as: Gupta S, Mahalingam K, Singh A, Selvan H, Somarajan BI, Gupta V. Posterior corneal morphological changes in primary congenital glaucoma. Indian J Ophthalmol 2022;70:2571-7.

Haag-Streit UK, Harlow, UK), cycloplegic refractive error, best corrected visual acuity, and corneal diameters were recorded. Homatropine 2% was used for cycloplegic refractive error assessment. Other corneal characteristics recorded included central corneal thickness and endothelial cell density in the treated arm. High-resolution anterior segment photos were taken (Eye Cap system; Haag Streit International, Koeniz, Switzerland) by an experienced observer.

This was followed by imaging of the cornea on high-resolution SDOCT (Spectralis, software version 6.5; Heidelberg Engineering, Heidelberg, Germany). Only those images with quality index of 25 dB or better were included for the analysis.[11] One eye of each patient was included in the study. The DM/pre-Descemet's layer (PDL) complex thickness was calculated using the ASOCT manual caliper tool with images zoomed at 400% magnification. An average of three readings was taken for areas both within and outside Haab's striae, making sure that the caliper was kept perpendicular to the endothelium. The subjective analysis of the data thus collected for involvement of DM, PDL, and other morphological characteristics was recorded.

Untreated PCG

Consecutive untreated PCG patients (age less than 5 years), scheduled for IOP-lowering surgery between Jan 2019 and Dec 2020, were recruited for the "untreated arm" of the study. Before the start of surgery, examination under anesthesia (sevoflurane) was performed. At this time, few intraoperative images were taken for PCG undergoing IOP-lowering surgery for the first time. ASOCT images across and along the Haab's striae were taken through microscope-integrated intraoperative OCT (iOCT machine) (Rescan 700 microscope-mounted OCT system; Carl Zeiss Meditec, Jena, Germany), unified into the Opmi Lumera 700 surgical microscope (Carl Zeiss Meditec).[12] Few snapshots of live recording were taken and interpreted by the glaucoma surgeon with respect to DM/PDL complex involvement. The Zeiss Callisto Eye provided an intraoperative surgical field on the left of the screen and a live optical coherence tomography (OCT) view on the right; the SDOCT images were recorded in "Cube" B scans in both horizontal and vertical orientations across the Haab's striae, which was the region of interest (ROI). A single surgeon assisted by the same observer controlled and recorded all the scans, so that the image quality and ROI could be standardized. The SDOCT scanning output was stored in the Callisto system for review.

The iOCT scanning was also performed for 10 treated patients who had been previously imaged on SDOCT, in order to validate if the differences seen in the two groups were due to differences in the resolution between the OCT machines. The images thus obtained on each of the OCT platforms (iOCT and Spectralis) were looked at subjectively for any visible differences in corneal profile.

The location and extent of Haab's striae were recorded for both the arms. Eyes with Haab's striae were categorized as those having central Haab's striae (within 4 mm of the pupillary axis), peripheral Haab's striae (outside 4 mm), and the third category having Haab's striae both at the center and periphery. To calculate the extent of Haab's striae, the diffuse illumination slit-lamp biomicroscopy clinical pictures for the treated arm and the intraoperative images for the untreated arm were reviewed on a freely available dynamic mathematics software "GeoGebra" (GeoGebra Team, Linz, Austria). For the treated arm, Haab's striae could be easily appreciated and measured, while for the untreated arm, the total extent of focal linear edema with or without perceptible tram-track appearance with confirmation on iOCT of diffuse intracameral posterior corneal bulge was considered as the total extent. To measure the degree of angular involvement (in peripheral Haab's striae), three points were marked using the angle tool: the first one at the edge of Haab's striae, the second at the center of pupil, and the last one on the edge of Haab's striae. The angle thus derived was divided by 30 to convert the extent into clock hours [Supplementary Fig. 1]. For measurement of the extent of central Haab's striae (using the same software), first the ends of Haab's striae were marked, then the segment was moved to periphery (near limbus), and then, angle subtended by it at the center of the pupil was measured.

Statistical analysis

The data were analyzed using Statistical Package for the Social Sciences (SPSS) software version 18.0 for Windows (SPSS Inc., Chicago, IL, USA). Kolmogorov–Smirnov test was used to verify normality distribution of continuous variables represented as mean ± standard deviation. Non-normal distribution was listed as median/interquartile range (IQR) and categorical variables as frequency (percentages). For continuous variables, the independent sample *t*-test or the Mann–Whitney U test was used and for categorical variables, the Chi-square test was used. The extent of Haab's striae was correlated with other parameters in a bivariate correlation and linear regression analysis. Pearson test was used for correlation analysis. P value < 0.05 was considered statistically significant.

Results

Of 145 children with PCG, we included 140 eyes that satisfied our inclusion criteria, 87 in the treated arm and 53 in the untreated arm. Five children in the treated group had to be excluded due to non-cooperation, low vision, nystagmus, and poor fixation. The demographic details of the subjects in treated and untreated arms are provided in Table 1.

Treated older PCG: A trabeculectomy with trabeculotomy or a goniotomy had been performed in the affected eyes for IOP control. The median spherical equivalent (SE) was − 3.25D with IQR of 4.8D (range: +0.50 to − 13.0 DS). The median visual acuity/IQR in logarithm of the minimum angle of resolution (LogMAR) was 0.83/0.60 (range: 0–2) [Table 1].

Untreated younger PCG: Ten out of 53 (20%) eyes had central Haab's striae, while 28 (53%) had involvement of both central as well as peripheral Haab's striae. Barring 17% eyes, all others had evidence of some degree of corneal edema and resultant haze.

Clinical appearance of Haab's striae

Table 2 provides the differences in posterior corneal morphology between the two groups.

Treated older PCG: Various patterns of Haab's striae were observed clinically on the slit lamp [Fig. 1a1–f1]. They ranged from those barely detectable clinically to small sectoral Haab's striae, ring Haab's striae extending circumferentially [Fig. 1a1], and from multiple Haab's striae within the same sector to

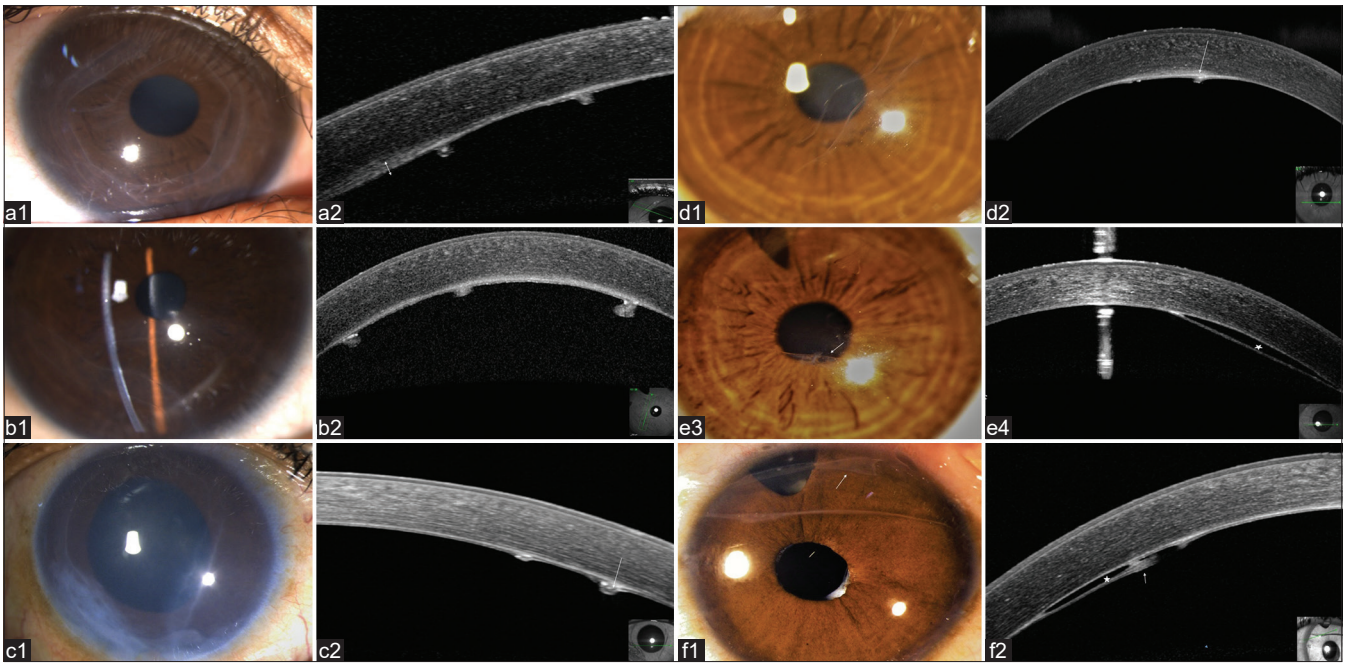

Figure 1: (Older treated PCG) Diffuse illumination slit-lamp biomicroscopy of the cornea with Haab's striae in different patients (a1–f1) with corresponding ASOCT scans through the same areas (a2–f2). (a1) Diffuse slit-lamp photographs showing circumferential ring Haab. (a2) Cross section through the Haab on ASOCT, depicting twin semi-circular protuberances and diffuse hyper-proliferation (double-headed arrow) of DM/PDL complex. (b1) Slit section through two tram tracks in another patient showing endothelial hyper-reflectivity both on slit illumination as well as on ASOCT. (b2) Intracameral mushroom-shaped protuberances as obtained on Spectralis (arrow aligned across Haab's striae). DM and PDL can be visualized as separate membranes. (c1, d1) Diffuse slit-lamp photographs of eyes with Haab's striae, with corneal decompensation occurring in c1. (c2, d2) ASOCT through Haab's striae depicting areas with overlying PDL breaks (arrows), inferonasal epithelial bullae visible in c2 within the inset. (e3, f1) Diffuse slit-lamp photographs of eyes with Haab's striae showing areas with folded membranes (arrows) within the tram tracks. (e4, f2) ASOCT through Haab's striae depicting DMD (stars) with adjacent areas of hyper-proliferative protuberances in f2. While dual membranes can be appreciated in areas outside DMD in (e2), the two membranes are well visualized within the detached complex in (f2). (Insets in (a2–f2) show the cross section across Haab's striae through which the ASOCT scans were taken). ASOCT = anterior segment optical coherence tomography, DM = Descemet's membrane, DMD = DM/PDL complex detachments, PCG = primary congenital glaucoma, PDL = pre-Descemet's layer

those crossing each other [Fig. 1a2]. Some of them appeared as membranes folded over themselves [Fig. 1e1, f1]. The average extent of Haab's striae was 5.52 ± 3.2 clock hours.

Untreated younger PCG: Borders of Haab's striae within the untreated arm were more often indistinct, associated with diffuse stromal haze, in contrast to their sharper demarcation in the treated arm [Fig. 2a1, b1]. In contrast to the typical tram-track pattern of the treated eyes, there was a crescentic opacification with focal corneal stromal and epithelial edema adjacent to the areas of Haab's striae in untreated eyes, usually accompanied by diffuse epithelial edema in areas distant from Haab's striae. Similar to that in the treated arm, the extent of Haab's striae ranged from small sectoral to those with ring Haab's striae extending circumferentially. The average extent of Haab's striae was 6.7 ± 2.8 clock hours.

ASOCT appearance of Haab's striae

Treated PCG

On ASOCT, the individual layers of the cornea overlying Haab's striae were evaluated. The observed manifestations were dual membrane appearance with hyper-reflectivity within both DM and PDL (86%), diffusely thickened DM/PDL complex with increased reflectivity (35%,) subtle excrescences or irregularities of DM/PDL complex in areas of Haab's striae (70%) [Fig. 1a2, b2], prominent intracameral protuberances of DM/PDL complex (usually twin) shaped differently as mushroom, trapezoid, or oval (92%) [Fig.1a2, b2], with (26%) or without (74%) visible breaks within the DM/PDL complex [Fig. 1c2, d2] and a chord-like membranous detachment involving the DM/PDL complex (8%) [Fig. 1e2, f2]. The DM/PDL complex thickness was increased significantly more within areas of Haab's striae (56.2 ± 22.6 μm) compared to regions without Haab's striae (33.2 ± 12.7 μm) ($P < 0.001$) [Table 1].

When the extent of Haab's striae was correlated with other parameters in a bivariate correlation and linear regression analysis, no correlation could be appreciated with most of the parameters. However, the extent of Haab's striae within the treated group was found to be significantly correlated with DM/PDL complex thickness within areas of Haab's striae (P: 0.008; β: 0.06). The DM/PDL complex was found to increase in thickness by 16.7 μm for each clock hour increase in the extent of Haab's striae.

Untreated younger PCG

On iOCT, underlying the areas of focal crescentic corneal edema, Haab's striae were appreciated as areas of focal mounds projecting intracamerally. DM and PDL were not identifiable as separate hyper-reflective membranes, rather as a diffuse hyper-reflective posterior cornea, sometimes with hyper-reflectivity reaching up to the lower half of corneal

Table 1: Demographic and clinical profile of the study group (*n*=140) along with corneal characteristics at the time of evaluation

Variable	Treated PCG	Untreated PCG	*P**
Number of eyes	87	53	
Male: female	60:27	38:15	0.7
Age of onset (months)	4.50/6.38 (0-60)	5.0/4.5 (0-47)	0.4
Age at examination (months)	132.0/72.0 (72-300)	8.7/6.1 (1-63)	**0.02**
Highest baseline IOP (mmHg)	31.81±6.11	38.20± 15.40	**0.05**
IOP at examination (mmHg)	16.00±4.86	28.50± 8.30	**0.002**
Spherical equivalent (D)	−3.25/4.78 (−10 to+3)	NA	-
Visual acuity (LogMAR)	0.83/0.60 (0-2)	NA	-
Corneal parameters			
Corneal diameter (mm)	13.61±0.86	13.10±0.46	**0.1**
Corneal clarity			**<0.001**
Clear cornea	63 (72.4)	9 (17.0)	
Mild corneal haze (visible iris details)	13 (14.9)	23 (43.4)	
Moderate corneal haze (slightly visible iris details)	7 (8.1)	13 (24.5)	
Severe corneal haze (not visible iris details)	4 (4.6)	8 (15.1)	
Central corneal thickness (µm)	529.71±64.12	617±76.3	**<0.001**
Number of eyes with Stromal edema	3 (7.5)	44 (83)	**<0.001**
DM/PDL complex thickness within HS (µm)	56.16±22.64	Not recorded	-
DM/PDL complex thickness outside HS (µm)	33.16±12.73	Not recorded	-
Location of HS			0.5
Central (within 4 mm of pupillary axis)	30 (34.5)	14 (26.4)	
Peripheral	44 (50.6)	28 (52.8)	
Both central and peripheral	13 (14.9)	11 (20.8)	
Extent of HS (clock hours)	5.52±2.20	6.70±2.80	**0.04**
Endothelial cell density (cells/mm^2) (*n*=63)#	1451.38± 289.77	Not recorded	

DM=Descemet's membrane, HS=Haab's striae, IOP=intraocular pressure, LogMAR=logarithm of the minimum angle of resolution, NA=not available, PCG=primary congenital glaucoma, PDL=pre-Descemet's membrane. *Data is represented as numbers (%), mean±standard deviation, or median/interquartile range. #Endothelial cell density was not possible in 24 patients with corneal haze.

stroma [Fig. 2a2, b2]. Twin protuberances, more diffuse in nature, could also be appreciated. Definite breaks within posterior corneal layers, subtle DM excrescences, or DM/PDL detachments (DMDs) could also not be appreciated. These eyes also showed corneal stromal and epithelial edema, more often. Hence, in untreated eyes, the diagnosis of Haab's striae was not established through visualization of posterior corneal breaks, but rather by the presence of hyper-reflective posterior Haab's striae protruding intracamerally as a diffuse mound or as twin protuberances.

In order to validate the agreement between the two different OCT machines, both Spectralis and iOCT scanning were performed in 10 treated eyes of older congenital glaucoma children. The iOCT gave similar morphological appearances within the posterior cornea as seen on Spectralis, thus validating the two machines [Supplementary Fig. 2].

Discussion

This study demonstrates that posterior cornea undergoes distinct morphological changes in eyes of children with PCG over time. On ASOCT, the treated eyes of older patients showed discrete circumscribed lesions representing areas of Haab's striae, in contrast to the diffuse appearance of the posterior corneal lesions in untreated eyes. Evidence from our series shows that following IOP-lowering surgery, Haab's striae undergo morphological variations, as was evident from difference in their appearance between the treated and untreated groups. Edema gives way to fibrosis, as apparent from more circumscribed appearance of the healed lesions. The opacified crescents give way to the pathognomonic tram-track appearance clinically, whereas on ASOCT, diffuse intracameral mounds give way to more circumscribed and discrete hyperproliferative protuberances within the edges of the DM tears. Singular hyper-reflective DM–PDL complex on ASOCT is replaced by dual hyper-reflective membranes, possibly due to posterior corneal fibrosis that encases both DM and PDL separately. Benito-Pascual *et al*.[7] described the protruding border of Haab's striae along with a thick tissue in between the two edges of Haab's striae. We found Haab's striae to appear as discrete intracameral outpouchings secondary to hyper-proliferation of both DM and PDL among older treated children. Morphologically, the shapes of Haab's striae varied from semi-circular, ovoid, and trapezoid to mushroom and linear patterns. It is difficult to ascertain the cause of this morphological heterogeneity, though it could be due to varying severity and time lapse since corneal stretch, as well as the differential healing response. The DM excrescences overlying areas of Haab's striae could possibly represent healing of smaller tears causing juxtaposition of DM edges soon after injury in eyes with controlled IOP. Surprisingly, we could not find an association between corneal diameters and the extent of Haab's striae.

We also observed DMDs in the posterior cornea in treated eyes. This could be due to an ongoing fibroproliferative response of the posterior cornea and secondary deposition of DM, such that localized subtle changes like tears in DM or PDL and detachments appeared. The DMDs could also be appreciated on slit-lamp microscopy (seven eyes in our series) as folded membranes within the tram-track pattern of the Haab's striae [Fig. 1e1, f1]. We had reported a large chord-like detachment in an adult patient who had been treated for PCG.[13] These detachments appear similar to type I DMD described by Dua *et al*.[14] in which both the PDL and DM detach together without an accompanying zone in between, suggesting that they might buckle and break together under

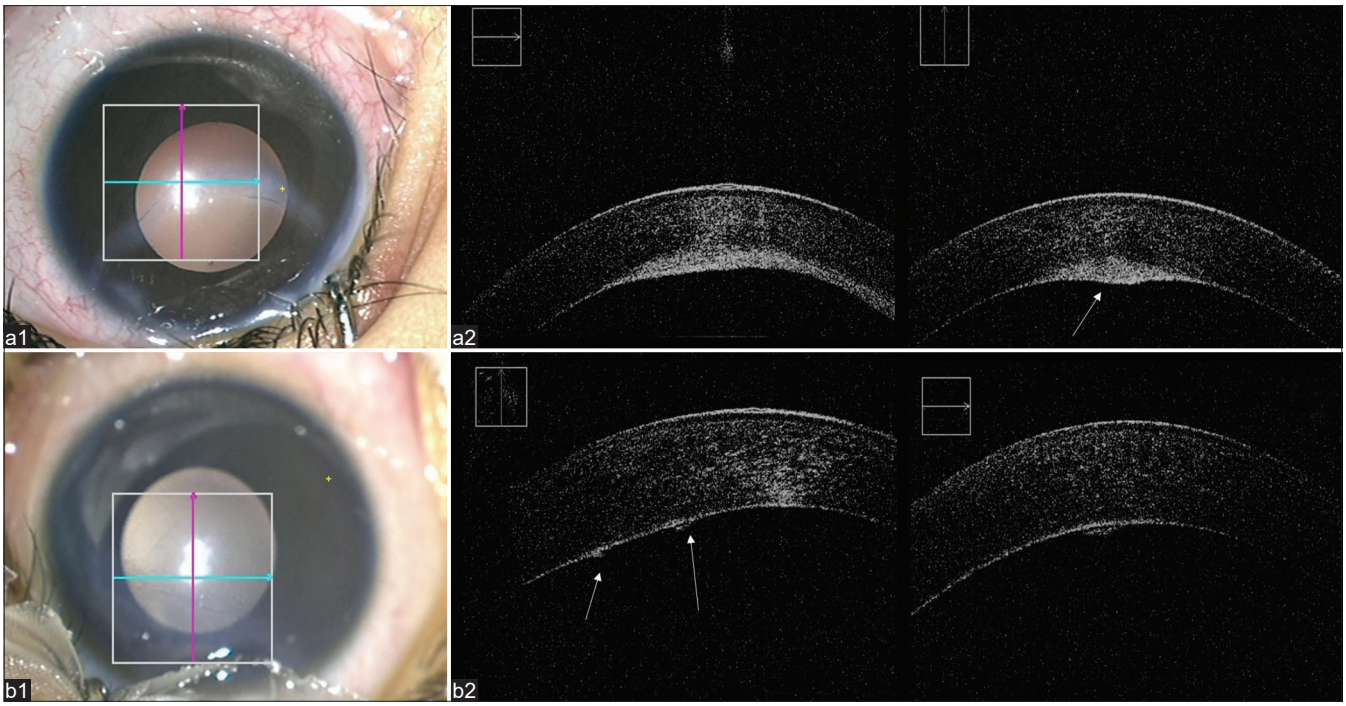

Figure 2: (a1, b1) Intraoperative diffuse illumination photographs of eyes of two children with primary congenital glaucoma taken just before proceeding for IOP-lowering surgery. Note crescentic opacification in both these eyes**.** (a2, b2) iOCT (right) scans show horizontal and vertical cross sections across the Haab's striae for both the children. Arrows indicate irregular, diffusely thickened posterior corneal contour without a clear demarcation between DM and PDL. DM = Descemet's membrane, iOCT = intraoperative optical coherence tomography, IOP = intraocular pressure, PDL = pre-Descemet's layer

pressure. Seepage of aqueous anteriorly through the DM/PDL complex break might cause DMD, followed subsequently by spontaneous healing, albeit persistent detachment. The other plausible etiology could be a tractional detachment, wherein elasticity disparity between anterior and posterior corneal layers (DM/PDL complex) causes failure of posterior corneal layers to stretch, examples of which have been seen as "isolated DM detachments" without break in adults with corneal hydrops.[15,16] Similar findings have been reported in a case of forceps-associated corneal injury in a neonate.[17]

Coexistence of PDL breaks along with DM tears within areas of Haab's striae was interesting and was not observed before in eyes of children with PDL. Involvement of PDL within areas of acute DM breaks has also been seen in eyes with keratoconus.[18] Parker *et al.* showed that a tear in DM by itself is not sufficient, and that a concomitant break in PDL is necessary for acute hydrops to set in.[18,19] On the contrary, acute hydrops in untreated PCG eyes heals on its own as soon as the DM/PDL breaks set in due to active proliferation at the edges acting to seal the discontinuity, ultimately bringing in the healing response.[5]

In this study, we observed an exaggerated thickening of DM/PDL complex within areas of Haab's striae, which was directly correlated with the extent of Haab's striae in treated eyes. We had previously reported both DM and PDL thickening in eyes with PCG *in vivo* as well as on histopathology.[20] The increased posterior corneal thickness represents a diffuse corneal response to the stretch injury/stress. Normally, basement membranes lose their elasticity[21] to gain thickness in response to higher stress conditions, among other factors,[22-24] which is an innate adaptation to enhance their tensile strength. During its initial exposure to high IOP, the elasticity of DM causes it to stretch,[25] with resultant simultaneous thickening, providing it higher biomechanical stab ility to prevent rupture. For rupturing human DM,[26] a mean threshold pressure of approximately 18 kPa is necessary,[27] resulting in development of DM tears beyond this. The anterior 40% of corneal stroma exhibits the highest cohesive tensile strength, thereafter plateauing at 40%–90% corneal stromal depth and then declining rapidly between the posterior 10% of the stroma (area also conforming to PDL) to DM.[28] The posterior 60% of the stroma is at least 50% weaker than the anterior stroma, with resultant heightened risks for breaks/ectasia/hydrops within the posterior stroma. Furthermore, nanomechanical measurements have shown that the anterior/epithelial surface of DM is stiffer than its posterior/intracameral surface,[29] implicating that DM may be more prone to breaks for an equivalent rise in IOP, when compared with PDL. Whether PDL breaks, such as those shown by us, are always associated with Haab's striae, whether they heal and auto-plug over time, whether their existence portends a poor prognosis for corneal clarity over time, and whether they augment corneal decompensation – the answers to these still elude us and would be worth investigating in a future study.

In our study, endothelial cell density was less in the treated PCG patients compared to normal population.[30] Gagnon *et al*.[31] proposed that the decrease in endothelial cell density in glaucoma patients could be due to direct damage from IOP, congenital endothelial alteration, or toxicity due to glaucoma medications.

Table 2: Posterior corneal morphological differences between the treated and untreated groups

Variable	Treated PCG (ASOCT) *n*=87	Untreated PCG (iOCT) *n*=53
Clinical appearance	Sharp borders, tram-track appearance, cornea often clear	Indistinct borders, diffuse crescentic opacification masking tram tracks
Barely detectable	Yes	Yes
Small sectoral	Yes	Yes
Ring HS	Yes	Yes
Multiple HS within the same sector	Yes	Yes
Membranes folded over themselves	Yes	No
ASOCT appearance		
Diffusely thickened/ hyper-reflective DM/ PDL complex (single membrane)	35%	100%
Other ASOCT features		
1. Dual membrane appearance	86%	-
2. Subtle excrescences	70%	-
3. Twin protuberances	92%	-
4. Visible DM/PDL breaks	26%	-

ASOCT=anterior segment optical coherence tomography, DM=Descemet's membrane, HS=Haab's striae, iOCT=intraoperative optical coherence tomography, PCG=primary congenital glaucoma, PDL=pre-Descemet's membrane

One of the limitations was that, for comparing the treated and untreated eyes, OCTs with different resolution were used (since younger patients were not cooperative for Spectralis ASOCT); the iOCT has a lower resolution (resolution 5 × 15 μm) compared to Spectralis SDOCT scans (resolution 3.5 × 7 μm). However, images of the same eyes using both machines revealed that morphological appearances on the two machines, for the same eye, were almost equivalent. Also, since the age ranges of the two groups were considerably different, they were not strictly comparable. Hence, a prospective evaluation following up the same children to look for temporal changes in the posterior cornea over years is planned to corroborate our study findings. Also, other variables like duration of raised IOP in children before treatment and effect of IOP on corneal biomechanics of pediatric eyes could be studied in future.

Conclusion

To summarize, this comparative study between eyes of children treated for PCG and untreated eyes showed distinct morphological differences between the two. Lowering of IOP limits the posterior corneal scarring and can impact the visual outcomes. Therapy in these children should be aimed not only at reducing IOP, but also to minimize fibrotic changes within the posterior cornea over time. Learning the pathogenesis of Haab's striae and knowing which layers of posterior cornea are involved can help us understand how to limit their extent and impact in future.

Financial support and sponsorship

Nil.

Conflicts of interest

There are no conflicts of interest.

References

1. Levy SG, Moss J, Sawada H, Dopping-Hepenstal PJ, McCartney AC. The composition of wide-spaced collagen in normal and diseased Descemet's membrane. Curr Eye Res 1996;15:45-52.
2. Fan Gaskin JC, Patel DV, McGhee CN. Acute corneal hydrops in keratoconus-new perspectives. Am J Ophthalmol 2014;157:921-8.
3. Szaflik JP, Oldak M, Kwiecien S, Udziela M, Szaflik J. Optical coherence tomography and *in vivo* confocal microscopy features of obstetric injury of the cornea. Cornea 2008;27:1070-3.
4. Yang B, Shao Y, Zhang M, Chen H. Imaging inadvertent Descemet's membrane break secondary to cataract surgery. Clin Exp Optom 2011;94:103-5.
5. Cibis GW, Tripathi RC. The differential diagnosis of Descemet's tears (Haab's striae) and posterior polymorpous dystrophy bands. A clinicopathologic study. Ophthalmology 1982;89:614-20.
6. Haab O. Atlas der äusseren Erkrankungen des Auges: Nebst Grundriss ihrer Pathologie und Therapie. JF Lehmann; 1899.
7. Benito-Pascual B, Pascual-Prieto J, Martinez-de-la-Casa JM, Saenz-Frances F, Santos-Bueso E. Haab striae: Optical coherence tomographic analysis. J Fr Ophtalmol 2019;42:11-5.
8. Mahelkova G, Filous A, Odehnal M, Cendelin J. Corneal changes assessed using confocal microscopy in patients with unilateral buphthalmos. Invest Ophthalmol Vis Sci 2013;54:4048-53.
9. Mastropasqua L, Carpineto P, Ciancaglini M, Nubile M, Doronzo E. *In vivo* confocal microscopy in primary congenital glaucoma with megalocornea. J Glaucoma 2002;11:83-9.
10. Pilat AV, Proudlock FA, Shah S, Sheth V, Purohit R, Abbot J, *et al*. Assessment of the anterior segment of patients with primary congenital glaucoma using handheld optical coherence tomography. Eye (Lond) 2019;33:1232-9.
11. Balasubramanian M, Bowd C, Vizzeri G, Weinreb RN, Zangwill LM. Effect of image quality on tissue thickness measurements obtained with spectral domain-optical coherence tomography. Opt Express 2009;17:4019-36.
12. Ehlers JP, Kaiser PK, Srivastava SK. Intraoperative optical coherence tomography using the RESCAN 700: Preliminary results from the DISCOVER study. Br J Ophthalmol 2014;98:1329-32.
13. Gupta S, Azmira K, Gupta V. A membrane in the eye. J Pediatr Ophthalmol Strabismus 2019;56:271.
14. Dua HS, Sinha R, D'Souza S, Potgieter F, Ross A, Kenawy M, *et al*. "Descemet Membrane Detachment": A novel concept in diagnosis and classification. Am J Ophthalmol 2020;218:84-98.
15. Basu S, Vaddavalli PK, Vemuganti GK, Ali MH, Murthy SI. Anterior segment optical coherence tomography features of acute corneal hydrops. Cornea 2012;31:479-85.
16. Ramamurthy B, Mittal V, Rani A, Ram M, Sangwan VS. Spontaneneous hydrops in pellucid marginal degeneration: Documentation by OCT-III. Clin Exp Ophthalmol 2006;34:616-7.
17. Kancherla S, Shue A, Pathan MF, Sylvester CL, Nischal KK. Management of Descemet membrane detachment after forceps birth injury. Cornea 2017;36:375-6.
18. Yahia Cherif H, Gueudry J, Afriat M, Delcampe A, Attal P, Gross H, *et al*. Efficacy and safety of pre-Descemet's membrane sutures for the management of acute corneal hydrops in keratoconus. Br J

Ophthalmol 2015;99:773-7.

19. Parker J, Birbal RS, van Dijk K, Oellerich S, Dapena I, Melles GR. Are Descemet membrane ruptures the root cause of corneal hydrops in keratoconic eyes? Am J Ophthalmol 2019;205:204-5.
20. Gupta S, Chaurasia AK, Sen S, Bhardwaj M, Mandal S, Titiyal JS, *et al*. The Descemet membrane in primary congenital glaucoma. Cornea 2021;40:172-8.
21. Welling L, Zupka M, Welling D. Mechanical properties of basement membrane. Physiology 1995;10:30-5.
22. Bruel A, Ortoft G, Oxlund H. Inhibition of cross-links in collagen is associated with reduced stiffness of the aorta in young rats. Atherosclerosis 1998;140:135-45.
23. Kiviranta P, Rieppo J, Korhonen RK, Julkunen P, Toyras J, Jurvelin JS. Collagen network primarily controls Poisson's ratio of bovine articular cartilage in compression. J Orthop Res 2006;24:690-9.
24. Krag S, Olsen T, Andreassen TT. Biomechanical characteristics of the human anterior lens capsule in relation to age. Invest Ophthalmol Vis Sci 1997;38:357-63.
25. Candiello J, Balasubramani M, Schreiber EM, Cole GJ, Mayer U, Halfter W, *et al*. Biomechanical properties of native basement membranes. FEBS J 2007;274:2897-908.
26. Danielsen CC. Tensile mechanical and creep properties of Descemet's membrane and lens capsule. Exp Eye Res 2004;79:343-50.
27. Jue B, Maurice DM. The mechanical properties of the rabbit and human cornea. J Biomech 1986;19:847-53.
28. Randleman JB, Dawson DG, Grossniklaus HE, McCarey BE, Edelhauser HF. Depth-dependent cohesive tensile strength in human donor corneas: Implications for refractive surgery. J Refract Surg 2008;24:S85-9.
29. Halfter W, Moes S, Halfter K, Schoenenberger MS, Monnier CA, Kalita J, *et al*. The human Descemet's membrane and lens capsule: Protein composition and biomechanical properties. Exp Eye Res 2020;201:108326.
30. Tamçelik N, Batu Oto B, Mergen B, Kiliçarslan O, Gönen B, Arici C. Corneal endothelial changes in patients with primary congenital glaucoma. J Glaucoma 2022;31:123-8.
31. Gagnon MM, Boisjoly HM, Brunette I, Charest M, Amyot M. Corneal endothelial cell density in glaucoma. Cornea 1997;16:314-8.

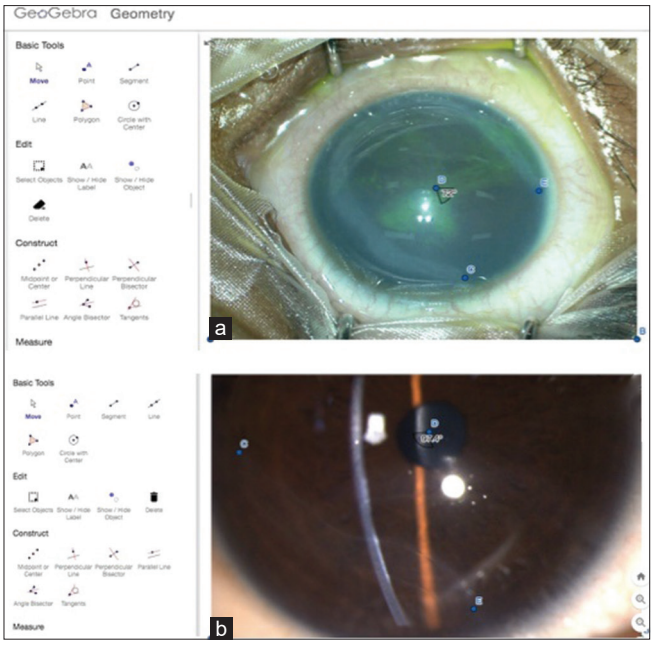

Supplementary Figure 1: (a) Image showing measurement of extent of Haab's striae (younger untreated PCG), using the angle measurement tool on GeoGebra software (360 – 72 = 288⌗). The clock hour equivalent is 9.6 (288/30). (b) Image showing measurement of extent of Haab's striae in older treated PCG (97.4⌗). The clock hour equivalent is 3.2 (97.4/30)PCG = primary congenital glaucoma

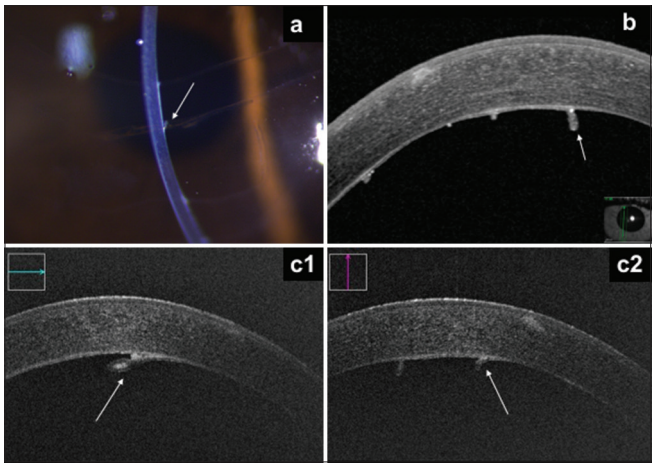

Supplementary Figure 2: The ASOCT scans of the same treated PCG patient on Spectralis as well as on iOCT. (a): Slit-lamp imaging of a patient with Haab's striae with slit section showing leaflet emerging from Haab under high magnification (arrow). (b) Spectralis shows multiple intracameral protuberances through the section across the Haab's striae; white arrow indicates the same leaflet as shown in (a). iOCT along the horizontal (c1) and vertical meridians (c2) across the Haab's striae. Inset shows the intraoperative photograph of the patient under retro-illumination. Dual discrete hyper-reflective membranes and circumscribed protuberances are visible. White arrow indicates the appearance of the leaflet as shown by arrows in (a) and (b)ASOCT = anterior segment optical coherence tomography, iOCT = intraoperative optical coherence tomography, PCG = primary congenital glaucoma